BJUI
BJU International

# Dishevelled segment polarity protein 3 (DVL3): a novel and easily applicable recurrence predictor in localised prostate adenocarcinoma

Pil-Jong Kim*, Ji Y. Park†, Hong-Gee Kim*, Yong Mee Cho‡ and Heounjeong Go‡

*Biomedical Knowledge Engineering Laboratory, Seoul National University School of Dentistry and Dental Research Institute, Seoul, †Department of Pathology, Catholic University of Daegu School of Medicine, Daegu, and ‡Department of Pathology, Asan Medical Center, University of Ulsan College of Medicine, Seoul, Korea

## Objective

To identify new biomarkers for biochemical recurrence (BCR) of prostate adenocarcinoma.

## Patients and Methods

Clinical information of 500 patients with prostate adenocarcinoma and their 152 RNA-sequencing and protein-array data from The Cancer Genome Atlas (TCGA) were separated into a discovery set and a validation set. Each dataset was analysed according to the Gleason grade groups reflecting BCR. The results obtained from the analysis using TCGA dataset were confirmed by immunohistochemistry analyses of a confirmation cohort composed of 395 patients with localised prostate adenocarcinoma.

## Results

TCGA discovery set was subgrouped into lower- and higher-risk groups for recurrence-free survival (RFS) ($P < 0.001$). Cyclin B1 (CCNB1), dishevelled segment polarity protein 3 (DVL3), paxillin (PXN), RAF1, transferrin, X-ray repair cross complementing 5 (XRCC5) and BIM had lower expression in the lower-risk group than that in the higher-risk group (all, $P < 0.05$). In TCGA validation set, CCNB1, DVL3, transferrin, XRCC5 and BIM were also differently expressed between the two groups. Immunohistochemically, DVL3 positivity was associated with high prostate-specific antigen (PSA) levels, resection margin involvement, and BCR (all, $P < 0.05$). A high Gleason score indicated a marginal relationship ($P = 0.055$). BIM positivity was related to high PSA levels, lymphovascular invasion, and BCR (all, $P < 0.05$). Both DVL3 positivity ($P = 0.010$) and BIM positivity ($P = 0.024$) were associated with shorter RFS, but statistical significance was lost when the multivariate Cox regression model included all patients. In the lower-risk group, the multivariate Cox model confirmed that DVL3 was an independent predictor for poor RFS (hazard ratio 1.80, $P = 0.040$), and the concordance index (*C*-index) was 0.805.

## Conclusions

DVL3 and BIM were expressed in patients with a higher risk of BCR. DVL3 may be a novel and easily applicable recurrence predictor of localised prostate adenocarcinoma.

## Keywords

dishevelled segment polarity protein 3, prostate adenocarcinoma, biochemical recurrence, immunohistochemistry, recurrence-free survival, #PCSM, #ProstateCancer

## Introduction

Prostate cancer is the second most common malignancy, with an estimated 1.1 million new cases in the world according to the GLOBOCAN 2012 report (http://globocan.iarc.fr). In the USA, prostate cancer is the second leading cause of cancer deaths in men, and 26 120 men were estimated to die from prostate cancer in 2016 [1]. More than 95% of all diagnosed cases of prostate cancer are prostate adenocarcinoma [2]. Prognostic factors of prostate adenocarcinoma serve to estimate the risk for disease progression and to determine treatment strategies [3]. Preoperative serum PSA level, Gleason score, pathological stage, and resection margin status are considered the most important prognosticators for recurrence and prostate cancer-specific mortality [3]. However, clinicopathological factors, such as PSA level, Gleason score and pathological stage, and imaging studies cannot provide a definite prediction of patient outcome. Biomarkers that are predictive of tumour aggressiveness and easily applicable can help make a more accurate therapeutic decision, particularly at the time of initial diagnosis, compared with clinical and histological variables [4].

 | doi:10.1111/bju.13783
Published by John Wiley & Sons Ltd. www.bjui.org

Although numerous promising biomarkers have been introduced that exhibit good discriminatory power, few can be assessed using easily applied methods, such as immunohistochemistry (IHC), in clinical practice [5–7].

The Cancer Genome Atlas (TCGA) is a public project led by the National Institutes of Health. TCGA has a goal of the discovery of major cancer-causing genomic alterations by creating a comprehensive atlas of cancer genomic profiles by systematising cancer genome data. To date, TCGA research teams have constructed large cohorts of >30 cancers using large-scale genome sequencing and integrated multi-dimensional analyses with phenotypic data. Coincidence studies of individual cancer types, as well as comprehensive pan-cancer analyses, have extended current knowledge of tumours [8,9]. TCGA provides clinicopathological, RNA, and protein data of each cancer. Reverse-phase protein array (RPPA) is a high-throughput antibody-based technique with a procedure similar to that of Western blots [10–12]. RPPA data can be coupled with clinical and mRNA expression data to consolidate the evidence of protein expression. RPPA data can also be confirmed using IHC [13].

In the present study, we analysed multi-dimensional proper omics data of prostate adenocarcinoma from the database of TCGA and sought to identify adequate IHC candidate targets to discriminate between patients with prostate adenocarcinoma according to the predictive recurrence of the tumours. We also confirmed expression of the candidates using IHC in a cohort of patients with prostate adenocarcinoma using available formalin-fixed paraffin-embedded (FFPE) tumour tissues.

## Patients and Methods

### TCGA mRNA and Protein Expression Data

We directly downloaded clinical information, level 3 RNA sequencing (RNA-seq) and RPPA data of 500 patients with prostate adenocarcinoma from the data portal of TCGA (https://tcga-data.nci.nih.gov) on 28 January 2016. Gene expression levels using RNA-Seq by Expectation Maximization (RSEM) normalised read counts were used for mRNA expression analysis. Text files of clinical data, mRNA, and protein obtained from each dataset were combined according to TCGA case identification. In all, 155 molecules with both mRNA and protein expression data were analysed in this study. The combined dataset was listed in chronological order and separated into two groups: 191 patients were included in the discovery set, and 309 patients were included in the validation set. The datasets were subgrouped and analysed according to the grade groups (GGs) or recurrence-free survival (RFS). The GGs were based on the Gleason score resulting in five prognostically distinct subgroups: GG1, Gleason score ≤6; GG2, Gleason score = 7 (3 + 4); GG3, Gleason score = 7 (4 + 3); GG4, Gleason score = 8 (3 + 5), (4 + 4), or (5 + 3); and GG5, Gleason score 9–10 [14]. Biochemical recurrence (BCR) was defined as a serum PSA level of ≥0.2 ng/mL on two consecutive occasions after achieving an undetectable PSA level after radical prostatectomy [15].

### FFPE Tumour Tissues and Tissue Microarray (TMA) Construction from Patients with Prostate Adenocarcinoma

To confirm the results obtained from TCGA data, we collected resected FFPE tumour tissues from 395 patients with prostate acinar adenocarcinoma who underwent radical prostatectomy at the Asan Medical Centre (AMC) from 1996 to 2006, designated as the AMC confirmation cohort. None of these patients received neoadjuvant or adjuvant androgen-deprivation treatments or had metastatic lesions at the time of surgery. Patient clinical information was acquired from electronic medical records. Pathological features, such as pathological diagnosis, Gleason score and pathological tumour (pT) stage, were reviewed according to the 2016 WHO Tumour Classification, the 2014 International Society of Urological Pathology (ISUP) Modified Gleason System, and the American Joint Committee on Cancer Staging System, 7th edition by two uropathologists (H.G. and Y.M.C.) [14,16,17].

A TMA with 0.6-mm diameter cores was generated from the collected tumour tissue blocks, and three representative cores were included for each case. This clinical study was approved by the Institutional Review Board of the AMC (2011-499).

### IHC

We attempted to validate the expression of all candidates from TCGA data with FFPE tumour tissues by IHC, but we could not evaluate cyclin B1 (CCNB1), paxillin (PXN), and X-ray repair cross complementing 5 (XRCC5) due to poor staining quality. The IHC detection of BIM, transferrin, RAF1 and dishevelled segment polarity protein 3 (DVL3) was conducted using specific antibodies. Sections from the TMA blocks were immunostained using the Ventana Benchmark XT automated staining system (Ventana Medical Systems, Tucson, AZ, USA) according to the manufacturer's protocol. Detailed antibody information and IHC conditions are summarised in Table S1.

The expression of all proteins as assessed by IHC was scored according to the visual intensity and the extent of staining. The protein expression level was quantitated using the H-score, which was calculated by multiplying the intensity and extent of each staining [18,19].

### Statistical Analyses

Statistical analyses were performed using R3.0.2 (R Development Core Team, Vienna, Austria). The relationships between groups were compared using the chi-squared test or Student's *t*-test. The Kaplan–Meier method with the log-rank test and multivariate Cox proportional hazards regression model were used to evaluate the effect of the classifier on patient survival. Multivariate survival analysis using Cox's regression model with a stepwise backward elimination approach was performed to acquire prognostic significant factors ($P < 0.1$) from features. To assess discrimination capability by expression levels of proteins for RFS in the final Cox proportional hazards regression model, Harrell's bias corrected concordance index (*C*-index) with models was refitted 1 000 times with the bootstrap resampling technique for the acquisition of the CIs. All statistical tests were two-sided, and statistical significance was defined as $P < 0.05$.

## Results

### Searching for Candidates in TCGA Data

We performed the log-rank test using RFS to determinate the threshold for subgrouping of the cases according to the GGs. Among 191 cases of the TCGA discovery set, the numbers of cases in GG1, GG2, GG3, GG4, and GG5 were 12, 85, 50, 20, and 24, respectively. The RFS was statistically distinctive in ≤GG2 vs ≥GG3 ($P = 0.002$), ≤GG3 vs ≥GG4 ($P < 0.001$), and ≤GG4 vs ≥GG5 ($P = 0.002$) (Table S2). Subgrouping was performed as ≤GG3 vs ≥GG4 because this grouping showed the lowest *P*-value, and were designated as the lower-risk and higher-risk groups for BCR. RFS was longer in the lower-risk group than in the higher-risk group, based on Kaplan–Meier survival analysis ($P < 0.001$) (Fig. 1). To identify candidate molecules implicated with clinicopathological and prognostic features of patients with prostate adenocarcinoma, RNA-seq mRNA and RPPA protein expression of molecules were compared in each subgroup using the Student's *t*-test. Seven molecules, including CCNB1, DVL3, PXN, RAF1, transferrin, XRCC5, and BIM, had differential mRNA and protein expression between the lower-risk and higher-risk groups in the TCGA discovery set (Table 1).

**Fig. 1** Kaplan–Meier curves obtained using the log-rank test showing RFS in patients with prostate adenocarcinoma in the lower-risk group vs the higher-risk group in TCGA discovery set (Days).

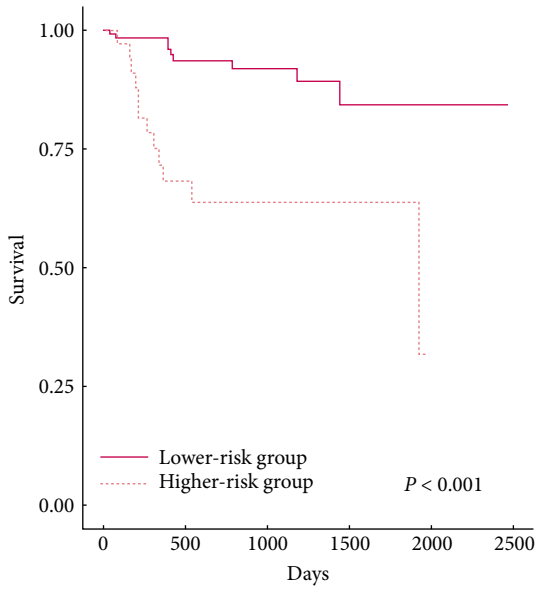


In the TCGA validation set, CCNB1, DVL3, transferrin, XRCC5 and BIM mRNA and protein were differently expressed between the two groups, and all of these genes exhibited increased expression in the higher-risk group compared with the lower-risk group, which is similar to that observed in the discovery set (Table 1). However, PXN and RAF1 protein expression lacked statistical significance.

### Confirming Protein Expression of the AMC Confirmation Cohort

The mean H-score of DVL3 was higher in only the higher-risk group compared with the lower-risk group ($P = 0.011$) (Table 1). DVL3 ($P = 0.009$) and BIM ($P = 0.023$) expression was associated with the RFS of patients, and the threshold H-scores were 88 and 15, respectively (Table 2 and Fig. 2A). RAF1 and transferrin had no correlation with the mean H-score or the RFS of patients between the groups. As summarised in Table 3, DVL3 positivity, i.e. H-score >88, was found in 67.3% (249/370), and BIM positivity, i.e. H-score >15, was found in 39.5% (156/395) of all patients. DVL3 expression was significantly associated with the presence of high PSA levels ($P = 0.030$), resection margin involvement ($P = 0.045$), and BCR ($P = 0.006$). High Gleason score, i.e. ≥GG4, exhibited a marginal relationship with DVL3 positivity ($P = 0.055$). However, DVL3 expression was not statistically related to age, pT stage, lymphovascular invasion (LVI), lymph node (LN) metastasis, or patient death. BIM expression was significantly associated with high PSA levels ($P = 0.022$), LVI ($P = 0.012$), and BCR ($P = 0.012$). However, BIM expression was not significantly related to age, GG, pT stage, resection margin involvement, LN metastasis, or patient death.

### Prognostic Implications of DVL3 and BIM Expression in the AMC Confirmation Cohort

DVL3 positivity was associated with shorter RFS in the univariate survival analysis [hazard ratio (HR) 1.73; $P = 0.010$], but its statistical significance was lost when the

 

**Table 1** mRNA and protein expression of the selected molecules.

| Molecules | TCGA discovery set | | | | TCGA validation set | | | | AMC confirmation cohort | |
|---|---|---|---|---|---|---|---|---|---|---|
| | RNA-seq | | RPPA | | RNA-seq | | RPPA | | IHC H-score† | |
| | logFC* | FDR | logFC | FDR | logFC | FDR | logFC | FDR | Mean (SD) lower- vs higher-risk | *P* |
| CCNB1 | 1.510 | 0.020 | 0.236 | 0.028 | 0.517 | <0.001 | 0.241 | <0.001 | NA | NA |
| DVL3 | 1.124 | 0.021 | 0.198 | 0.022 | 0.193 | <0.001 | 0.150 | <0.001 | 121 (70) vs 144 (69) | 0.011 |
| PXN | 0.861 | 0.032 | 0.204 | 0.036 | –0.185 | 0.001 | 0.009 | 0.874 | NA | NA |
| RAF1 | 1.155 | 0.020 | 0.186 | 0.037 | 0.141 | <0.001 | 0.036 | 0.240 | 189 (55) vs 187 (56) | 0.725 |
| Transferrin | 1.269 | 0.046 | 0.370 | 0.028 | 0.327 | <0.001 | 0.345 | <0.001 | 17 (37) vs 25 (39) | 0.130 |
| XRCC5 | 1.106 | 0.020 | 0.222 | 0.028 | 0.074 | 0.031 | 0.220 | <0.001 | NA | NA |
| BIM | 1.204 | 0.020 | 0.263 | 0.011 | 0.248 | <0.001 | 0.227 | <0.001 | 41 (60) vs 50 (61) | 0.242 |

*logFC, log fold change; FDR, false discovery rate; NA, not applicable. *logFC was used to compare the expression levels of RNA-seq mRNA and RPPA protein between the lower- and higher-risk groups. †H-score ranged from 0 to 300. The mean H-scores of DVL3, RAF1, transferrin, and BIM were 126, 188, 19, and 43, respectively, in all patients in the AMC confirmation cohort.*

**Table 2** The best thresholds of H-score determined using IHC reflecting BCR in patients in the AMC confirmation cohort.

| Molecules | Threshold (H-score) | *P* |
|---|---|---|
| DVL3 | 88 | 0.009 |
| RAF1 | 248 | 0.131 |
| Transferrin | 82 | 0.094 |
| BIM | 15 | 0.023 |

multivariate Cox regression model included all patients (Table S3). In the lower-risk group, patients with DVL3 positivity had reduced RFS compared with those with DVL3 negativity by both Kaplan–Meier ($P = 0.012$; Fig. 2B) and univariate Cox regression (HR 2.00, $P = 0.014$) analyses. Importantly, the multivariate Cox regression model comprising DVL3, age, PSA level, and pT stage in the lower-risk group confirmed that DVL3 was a significant independent predictor of poor RFS (HR 1.80, $P = 0.040$) (Table 4). The *C*-index of the Cox regression model comprising age, PSA level, and pT stage was 0.756 (95% CI 0.708–0.804). When DVL3 was added to the model, the *C*-index was increased by 0.049, and the *C*-index was 0.805 (95% CI: 0.755–0.855). In the higher-risk group, patients with DVL3 positivity were not associated with RFS ($P = 0.850$; Fig. 2C).

BIM positivity was associated with reduced RFS by univariate survival analysis ($P = 0.023$ via Kaplan–Meier analysis; HR 1.48, $P = 0.024$ via Cox regression analysis), but its statistical significance was lost when the multivariate Cox regression model included all patients (Fig. 3A and Table S4), similar to DVL3. In addition, BIM expression was not related to RFS in the lower-risk or the higher-risk groups (Fig. 3B and C).

## Discussion

The incidence of clinically diagnosed prostate cancer rapidly increased worldwide from the late 1980s to the early 2000s as

**Fig. 2** Kaplan–Meier curves obtained using the log-rank test showing the RFS of patients with prostate adenocarcinoma with positive vs negative expression of DVL3. (**A**) All patients; (**B**) Lower-risk group patients; (**C**) Higher-risk group patients.

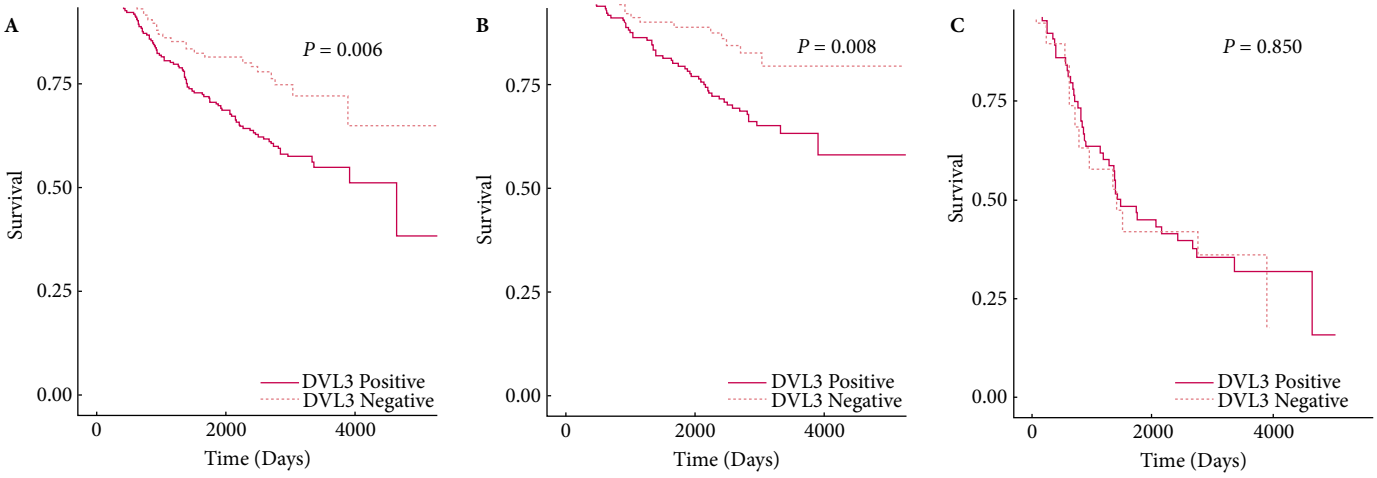

**Table 3** Association of DVL3 and BIM expression with clinicopathological features of patients in the AMC confirmation cohort.

| | *N* (%) | | | | | | | |
|---|---|---|---|---|---|---|---|---|
| | DVL3 | | | | BIM | | | |
| | Total (*N* = 370) | Negative (*N* = 121) | Positive (*N* = 249) | *P* | Total (*N* = 395) | Negative (*N* = 239) | Positive (*N* = 156) | *P* |
| Age, years | | | | | | | | |
| <60 | 75 | 25 (33.3) | 50 (66.7) | 1.000 | 83 | 50 (60.2) | 33 (39.8) | 1.000 |
| ≥60 | 295 | 96 (32.5) | 199 (67.5) | | 312 | 189 (60.6) | 123 (39.4) | |
| PSA, ng/mL | | | | | | | | |
| <10 | 223 | 83 (37.2) | 140 (62.8) | 0.030 | 239 | 156 (65.3) | 83 (34.7) | 0.022 |
| ≥10 | 147 | 38 (25.9) | 109 (74.1) | | 156 | 83 (53.2) | 73 (46.8) | |
| GG | | | | | | | | |
| ≤3 | 285 | 101 (35.4) | 184 (64.6) | 0.055 | 306 | 192 (62.7) | 114 (37.3) | 0.118 |
| ≥4 | 85 | 20 (23.5) | 65 (76.5) | | 89 | 47 (52.8) | 42 (47.2) | |
| pT stage | | | | | | | | |
| 2 | 203 | 74 (36.5) | 129 (63.5) | 0.113 | 216 | 139 (64.4) | 77 (35.6) | 0.107 |
| 3, 4 | 167 | 47 (28.1) | 120 (71.9) | | 179 | 100 (55.9) | 79 (44.1) | |
| LVI | | | | | | | | |
| Absent | 306 | 104 (34.0) | 202 (66.0) | 0.315 | 326 | 207 (63.5) | 119 (36.5) | 0.012 |
| Present | 64 | 17 (26.6) | 47 (73.4) | | 69 | 32 (46.4) | 37 (53.6) | |
| Resection margin involvement | | | | | | | | |
| Absent | 264 | 95 (36.0) | 169 (64.0) | 0.045 | 281 | 174 (61.9) | 107 (38.1) | 0.430 |
| Present | 106 | 26 (24.5) | 80 (75.5) | | 114 | 65 (57.0) | 49 (43.0) | |
| LN metastasis | | | | | | | | |
| Absent | 337 | 114 (33.8) | 223 (66.2) | 0.215 | 361 | 224 (62.0) | 137 (38.0) | 0.069 |
| Present | 29 | 6 (20.7) | 23 (9.3) | | 30 | 13 (43.3) | 17 (56.7) | |
| Death | | | | | | | | |
| Absent | 295 | 94 (31.9) | 201 (68.1) | 0.587 | 316 | 196 (62.0) | 120 (38.0) | 0.269 |
| Present | 75 | 27 (36.0) | 48 (64.0) | | 79 | 43 (54.4) | 36 (45.6) | |
| Cancer-specific death | | | | | | | | |
| Absent | 359 | 118 (32.9) | 241 (67.1) | 0.949 | 382 | 234 (61.3) | 148 (38.7) | 0.172 |
| Present | 11 | 3 (27.3) | 8 (72.7) | | 13 | 5 (38.5) | 8 (61.5) | |
| BCR | | | | | | | | |
| Absent | 244 | 92 (37.7) | 152 (62.3) | 0.006 | 261 | 170 (65.1) | 91 (34.9) | 0.012 |
| Present | 126 | 29 (23.0) | 97 (77.0) | | 134 | 69 (51.5) | 65 (48.5) | |

*pT stage, pathological T stage.*

**Table 4** Multivariate Cox proportional hazard regression model including DVL3 for RFS of the lower-risk group in the AMC confirmation cohort.

| Feature | Standard | Univariate | | Multivariate | |
|---|---|---|---|---|---|
| | | HR (95% CI) | *P* | HR (95% CI) | *P* |
| DVL3 | Positive vs negative | 2.00 (1.15–3.50) | 0.014 | 1.80 (1.03–3.17) | 0.040 |
| Age, years | ≥60 vs <60 | 0.63 (0.39–1.02) | 0.058 | 0.55 (0.33–0.90) | 0.018 |
| LVI | Present vs absent | 2.31 (1.35–3.95) | 0.002 | | |
| LN metastasis | Present vs absent | 2.94 (1.28–6.75) | 0.011 | | |
| RM involvement | Present vs absent | 2.82 (1.82–4.37) | <0.001 | | |
| PSA, ng/mL | ≥10 vs <10 | 4.37 (2.78–6.86) | <0.001 | 3.44 (2.08–5.68) | <0.001 |
| pT stage | 3, 4 vs 2 | 4.00 (2.53–6.32) | <0.001 | 2.70 (1.62–4.50) | <0.001 |

*RM, resection margin; pT stage, pathological T stage.*

a result of the adoption of serum PSA screening (http://globocan.iarc.fr). Several molecular alterations based on the pathognomonics of the tumours have markedly improved the management of patients and have even change the classification of tumour subtypes. For example, the detection of activating mutations in the epidermal growth factor receptor (*EGFR*) tyrosine kinase domain in patients with advanced non-small-cell lung cancer has allowed clinicians to efficiently apply EGFR-targeted therapy [20]. Renal cell carcinoma that harbours gene fusions involving two members i.e. transcription factor E3 (*TFE3*) and transcription factor EB (*TFEB*), of the micropthalmia (MiT) family of transcription factors exhibits unique clinicopathological features and is subtyped in a distinctive entity [21]. In prostate cancer, several molecular aberrations, such as alterations of the androgen receptor or erythroblast transformation-specific (ETS)-related gene (*ERG*) overexpression, are commonly regarded as potential biomarkers, but their predictive or

**Fig. 3** Kaplan–Meier curves obtained using the log-rank test showing the RFS of patients with prostate adenocarcinoma with positive vs negative expression of BIM. (**A**) All patients; (**B**) Lower-risk group patients; (**C**) Higher-risk group patients.

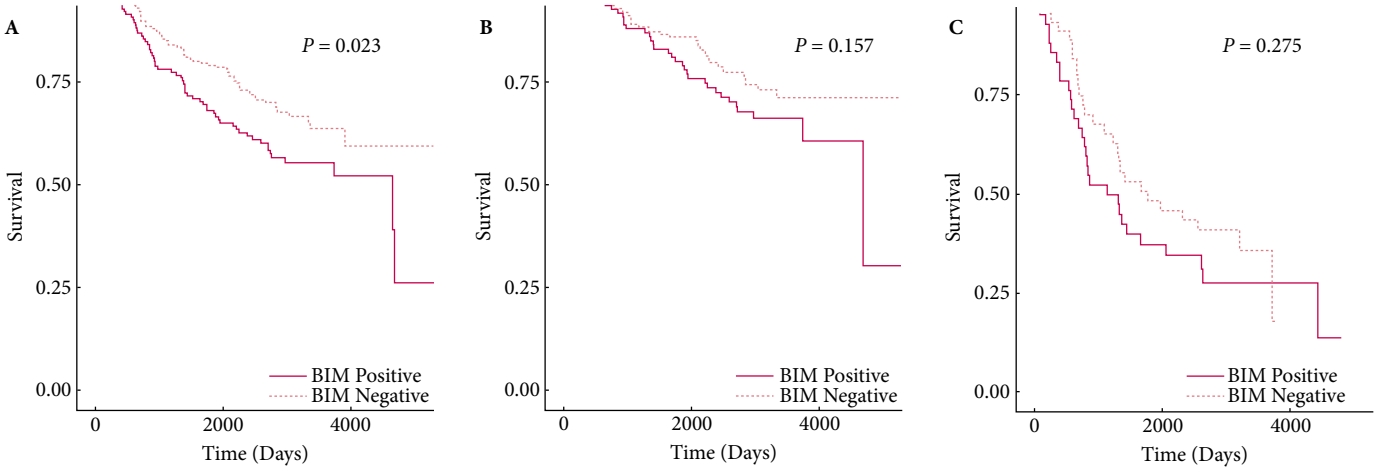


prognostic values remain disputed. Androgen signalling aberrations occur later in tumour progression, and the prognostic value of transmembrane protease, serine 2 (*TMPRSS2*)-*ERG* is limited in radical prostatectomy specimens [22,23]. Therefore, efforts to discover novel biomarkers that are clinically applicable are still ongoing, particularly to prevent over- or under-treatment in patients with localised prostate adenocarcinoma who undergo radical prostatectomy.

In the present study, we investigated new prognostic biomarker candidates for tumour recurrence. All the candidate molecules are involved in cancer progression regulating proliferation, mitosis, DNA repair, invasion, metastasis, angiogenesis, molecular transportation and apoptosis. CCNB1 regulates mitosis, especially G2/M phase. In prostate cancer, knockdown of tripartite motif 59 (TRIM59), which is a regulator of transcription factors and tumour suppressors, inhibited cell proliferation and colony formation. The cell cycle regulators cell division cycle 25A (CDC25A), cyclin dependent kinase 1 (CDK1), and CCNB1 were also decreased by TRIM59 short hairpin RNA-mediated knockdown [24]. XRCC5 functions in the repair of DNA double-strand breaks. Variable number tandem repeats polymorphism in the XRCC5 promoter is associated with altered risk of breast cancer in breast cancer type 1 susceptibility protein (*BRCA1*)+ and breast cancer type 2 susceptibility protein (*BRCA2*)+ carriers [25]. Glucose deprivation mediated stress increased the expression of nuclear Ku encoded by XRCC5 or XRCC6 and resistance to radiation-induced oxidative stress in HT29 and DU145 human prostate cancer cells [26].

We showed that DVL3 expression correlated with important clinicopathological variables, such as serum PSA level and Gleason score. DVL3 was also related to poor RFS. Particularly, in the patients with GG1–GG3 prostate adenocarcinoma, DVL3 was an independent prognostic factor for BCR according to the multivariate Cox model comprising age, PSA level, and pT stage with a high *C*-index. Currently, no definite and easily applicable biomarkers for BCR, in addition to age, serum PSA level, and several histological variables, such as pT stage, resection margin involvement, and high-grade prostatic intraepithelial neoplasia, have been suggested in this group of patients [3,7]. Consequently, DVL3 information may aid in clinical decision-making, such as follow-up interval or implementing adjuvant treatment. In addition, in the multivariate Cox regression model of all cases, DVL3 was not an independent predictive factor, potentially due to the correlation with resection margin involvement, PSA level, and Gleason score. Dysregulation of Wnt signalling has been shown in several types of cancers, including prostate cancer [27]. DVLs are dishevelled segment polarity proteins that are a homologue of the *Drosophila dishevelled (dsh)* gene and encode a cytoplasmic phosphoprotein that regulates cell proliferation by Wnt signalling [27]. DVL3, a member of DVLs family and plays an important role in signal amplification in the canonical Wnt/β-catenin cascade during tumorigenesis [28]. In addition, DVL3 transduces extracellular polarity cues and integrates a myriad of extracellular and intracellular inputs to induce intracellular cytoskeleton rearrangements and impact cell behaviours as a member of the non-canonical Wnt/planar cell polarity pathway [29]. Also, DVL3 regulates cancer progression, invasion, metastasis, and angiogenesis, and the overexpression of DVL3 correlates with progression in patients with non-small-cell lung cancer [30]. Recently, DVL3 was suggested to mediate resistance to the inhibition of IGF receptor-1 (IGF-IR), which is a promising new therapeutic target for several cancers including breast and prostate cancers in preclinical and early trials, by mediating the IGF-

RAS signalling pathway. Predictive biomarkers for response to IGF-IR-targeted therapy have not been developed yet. Moreover, sensitivity to IGF-IR inhibition was specifically enhanced by genetic or pharmacological blockade of DVL3 [31]. These results suggest that DVL3 may have predictive value or be a novel therapeutic target in addition to having prognostic value.

Transferrin is involved in cellular iron transportation by receptor-mediated endocytosis. Recently, transferrin has been used as an efficient carrier of therapeutic molecules to overcome drug resistance in many cancers such as breast cancer, lung cancer or glioblastoma [32–34]. BIM acts as an apoptotic activator and its expression is associated with good prognosis in colon cancer [35]. In the present study, the expression of both transferrin and BIM were increased in the higher-risk group compared to the lower-risk group and the implications should be investigated in further studies.

We analysed TCGA data by integrating clinical, mRNA and protein expression to overcome the limited number of cohorts. RPPA is a protein array of a micro- or nano-scaled dot-blot platform that is printed to a substrate to simultaneously measure protein expression levels in a large number of biological samples in a quantitative manner [36]. Human epidermal growth factor receptor 2 (HER2) scores based on IHC were reproduced using RPPA with breast cancer FFPE tissues, and programmed death-ligand 1 (PD-L1) mRNA expression exhibited a positive correlation with RPPA data in lung adenocarcinoma [13,37]. However, the list of evaluated molecules by RPPA in TCGA were limited to only a few hundred proteins. Thus, there is a possibility that a valuable candidate has been missed. The present study can be extended when new TCGA RPPA data for new molecules are added. In addition, the results of DVL3 IHC should be validated with biopsy or whole resection specimen because the expression pattern may vary depending on the type of specimen and heterogeneity of the tumour.

We identified candidate biomarkers of BCR of prostate adenocarcinoma by integrating the RPPA and mRNA data from TCGA. Then, these biomarkers were validated using IHC in a prostate adenocarcinoma confirmation cohort, and both DVL3 and BIM were associated with BCR. Importantly, DVL3 may be a novel and easily applicable recurrence predictor of localised prostate adenocarcinoma.

## Acknowledgements

This research was supported by Basic Science Research Program through the National Research Foundation of Korea (NRF) funded by the Ministry of Science, ICT and future Planning (NRF-2014R1A2A1A11049728).

## Conflicts of Interest

None.

## References

1 **American Cancer Society.** Cancer Facts & Figures, 2016. Available at: http://www.cancer.org/research/cancer-facts-statistics/all-cancer-facts-figures/cancer-facts-figures-2016.html. Accessed January 2017

2 **Humphrey PA**. *Prostate Pathology*. Chicago: American Society for Clinical Pathology, 2003

3 **Eble J, Epstein J, Sesterhenn I, Sauter, G eds.** *WHO Classification of Tumours: Pathology and Genetics of Tumours of the Urinary System and Male Genital Organs (IARC WHO Classification of Tumours)*. Lyon, France: International Agency for Research on Cancer (IARC) Press, 2004.

4 **Kristiansen G**. Diagnostic and prognostic molecular biomarkers for prostate cancer. *Histopathology* 2012; 60: 125–41

5 **Queisser A, Hagedorn SA, Braun M, Vogel W, Duensing S, Perner S**. Comparison of different prostatic markers in lymph node and distant metastases of prostate cancer. *Mod Pathol* 2015; 28: 138–45

6 **Huber F, Montani M, Sulser T et al.** Comprehensive validation of published immunohistochemical prognostic biomarkers of prostate cancer -what has gone wrong? A blueprint for the way forward in biomarker studies. *Br J Cancer* 2015; 112: 140–8

7 **Crawford ED, Ventii K, Shore ND**. New biomarkers in prostate cancer. *Oncology (Williston Park)* 2014; 28: 135–42

8 **Chin L, Andersen JN, Futreal PA**. Cancer genomics: from discovery science to personalized medicine. *Nat Med* 2011; 17: 297–303

9 **Tomczak K, Czerwinska P, Wiznerowicz M**. The Cancer Genome Atlas (TCGA): an immeasurable source of knowledge. *Contemp Oncol (Pozn)* 2015; 19: A68–77

10 **Paweletz CP, Charboneau L, Bichsel VE et al.** Reverse phase protein microarrays which capture disease progression show activation of pro-survival pathways at the cancer invasion front. *Oncogene* 2001;20:1981–9.

11 **Nishizuka S, Charboneau L, Young L et al.** Proteomic profiling of the NCI-60 cancer cell lines using new high-density reverse-phase lysate microarrays. *Proc Natl Acad Sci USA* 2003; 100: 14229–34

12 **Tibes R, Qiu Y, Lu Y et al.** Reverse phase protein array: validation of a novel proteomic technology and utility for analysis of primary leukemia specimens and hematopoietic stem cells. *Mol Cancer Ther* 2006; 5: 2512–21

13 **Assadi M, Lamerz J, Jarutat T et al.** Multiple protein analysis of formalin-fixed and paraffin-embedded tissue samples with reverse phase protein arrays. *Mol Cell Proteomics* 2013; 12: 2615–22

14 **Epstein JI, Egevad L, Amin MB, Delahunt B, Srigley JR, Humphrey PA**. The 2014 International Society of Urological Pathology (ISUP) Consensus Conference on Gleason Grading of Prostatic Carcinoma: definition of Grading Patterns and Proposal for a New Grading System. *Am J Surg Pathol* 2016;40:244–52.

15 **Cookson MS, Aus G, Burnett AL et al.** Variation in the definition of biochemical recurrence in patients treated for localized prostate cancer: the American Urological Association Prostate Guidelines for Localized Prostate Cancer Update Panel report and recommendations for a standard in the reporting of surgical outcomes. *J Urol* 2007; 177: 540–5

16 **Epstein JI, Allsbrook WC Jr, Amin MB, Egevad LL, Committee IG**. The 2005 International Society of Urological Pathology (ISUP) consensus conference on Gleason grading of prostatic carcinoma. *Am J Surg Pathol* 2005; 29: 1228–42

17 **Edge SB, Compton CC**. The American Joint Committee on Cancer: the 7th Edition of the AJCC Cancer Staging Manual and the Future of TNM. *Ann Surg Oncol* 2010; 17: 1471–4

 

18 **John T, Liu G, Tsao MS.** Overview of molecular testing in non-small-cell lung cancer: mutational analysis, gene copy number, protein expression and other biomarkers of EGFR for the prediction of response to tyrosine kinase inhibitors. *Oncogene* 2009; 28(Suppl. 1): S14–23

19 **Pirker R, Pereira JR, von Pawel J et al.** EGFR expression as a predictor of survival for first-line chemotherapy plus cetuximab in patients with advanced non-small-cell lung cancer: analysis of data from the phase 3 FLEX study. *Lancet Oncol* 2012; 13: 33–42

20 **Paleiron N, Bylicki O, Andre M et al.** Targeted therapy for localized non-small-cell lung cancer: a review. *Onco Targets Ther* 2016; 9: 4099–104

21 **Argani P.** MiT family translocation renal cell carcinoma. *Semin Diagn Pathol* 2015; 32: 103–13

22 **Pettersson A, Graff RE, Bauer SR et al.** The TMPRSS2:ERG rearrangement, ERG expression, and prostate cancer outcomes: a cohort study and meta-analysis. *Cancer Epidemiol Biomarkers Prev* 2012; 21: 1497–509

23 **Saraon P, Jarvi K, Diamandis EP.** Molecular alterations during progression of prostate cancer to androgen independence. *Clin Chem* 2011; 57: 1366–75

24 **Lin WY, Wang H, Song X et al.** Knockdown of tripartite motif 59 (TRIM59) inhibits tumor growth in prostate cancer. *Eur Rev Med Pharmacol Sci* 2016; 20: 4864–73

25 **Cui J, Luo J, Kim YC et al.** Differences of variable number tandem repeats in XRCC5 promoter are associated with increased or decreased risk of breast cancer in BRCA gene mutation carriers. *Front Oncol* 2016; 6: 92

26 **Li J, Ayene R, Ward KM, Dayanandam E, Ayene IS.** Glucose deprivation increases nuclear DNA repair protein Ku and resistance to radiation induced oxidative stress in human cancer cells. *Cell Biochem Funct* 2009; 27: 93–101

27 **Kypta RM, Waxman J.** Wnt/beta-catenin signalling in prostate cancer. *Nat Rev Urol* 2012; 9: 418–28

28 **Mohammed MK, Shao C, Wang J et al.** Wnt/β-catenin signaling plays an ever-expanding role in stem cell self-renewal, tumorigenesis and cancer chemoresistance. *Genes Dis* 2016; 3: 11–40

29 **Wang Y.** Wnt/Planar cell polarity signaling: a new paradigm for cancer therapy. *Mol Cancer Ther* 2009; 8: 2103–9

30 **Uematsu K, He B, You L, Xu Z, McCormick F, Jablons DM.** Activation of the Wnt pathway in non-small cell lung cancer: evidence of dishevelled overexpression. *Oncogene* 2003; 22: 7218–21

31 **Gao S, Bajrami I, Verrill C et al.** Dsh homolog DVL3 mediates resistance to IGFIR inhibition by regulating IGF-RAS signaling. *Cancer Res* 2014; 74: 5866–77

32 **Wadajkar AS, Dancy JG, Hersh DS et al.** Tumor-targeted nanotherapeutics: overcoming treatment barriers for glioblastoma. *Wiley Interdiscip Rev Nanomed Nanobiotechnol* 2016. [Epub ahead of print]. doi: 10.1002/wnan.1439

33 **Zhang B, Zhang Y, Yu D.** Lung cancer gene therapy: transferrin and hyaluronic acid dual ligand-decorated novel lipid carriers for targeted gene delivery. *Oncol Rep* 2017; 37: 937–44

34 **He YJ, Xing L, Cui PF et al.** Transferrin-inspired vehicles based on pH-responsive coordination bond to combat multidrug-resistant breast cancer. *Biomaterials* 2017; 113: 266–78

35 **Sinicrope FA, Rego RL, Okumura K et al.** Prognostic impact of bim, puma, and noxa expression in human colon carcinomas. *Clin Cancer Res* 2008; 14: 5810–8

36 **Spurrier B, Ramalingam S, Nishizuka S.** Reverse-phase protein lysate microarrays for cell signaling analysis. *Nat Protoc* 2008; 3: 1796–808

37 **Lou Y, Diao L, Cuentas ER et al.** Epithelial-mesenchymal transition is associated with a distinct tumor microenvironment including elevation of inflammatory signals and multiple immune checkpoints in lung Adenocarcinoma. *Clin Cancer Res* 2016; 22: 3630–42



Correspondence: Heounjeong Go, Department of Pathology, University of Ulsan College of Medicine, Asan Medical Center,88, Olympic-ro 43-gil, Songpa-gu, Seoul 05505, Korea.

e-mail: damul37@amc.seoul.kr


Abbreviations: AMC, Asan Medical Centre; BCR, biochemical recurrence; CCNB1, cyclin B1; *C*-index, concordance index; DVL3, dishevelled segment polarity protein 3; EGFR, epidermal growth factor receptor; ERG, erythroblast transformation-specific (ETS)-related gene; FFPE, formalin-fixed paraffin-embedded; HR, hazard ratio; IGF-IR, IGF receptor-1; IHC, immunohistochemistry; LN, lymph node; LVI, lymphovascular invasion; PXN, paxillin; RFS, recurrence-free survival; RNA-seq, RNA sequencing; RPPA, reverse-phase protein array; TCGA, The Cancer Genome Atlas; TMA, tissue microarray; TRIM59, tripartite motif 59; XRCC5, X-ray repair cross complementing 5.

## Supporting Information

Additional Supporting Information may be found in the online version of this article:

**Table S1** List of antibodies and conditions used for IHC.
**Table S2** Log-rank test of RFS in subgroupings according to the GGs in the TCGA discovery set.
**Table S3** Multivariate Cox proportional hazard regression model including DVL3 for RFS in all patients in the AMC cohort.
**Table S4** Multivariate Cox proportional hazard regression model including BIM for recurrence-free survival of all patients in the AMC confirmation cohort.